

Efficient optical pulse compression using chalcogenide single-mode fibers

Libin Fu, Alexander Fuerbach, Ian C. M. Littler, and Benjamin J. Eggleton
*Center for Ultrahigh-bandwidth Devices for Optical Systems (CUDOS), School of Physics,
 University of Sydney, NSW 2006, Australia*

(Received 5 October 2005; accepted 15 January 2006; published online 24 February 2006)

We demonstrate compression of low-power 6 ps pulses to 420 fs around 1550 nm in a compact all-fiber scheme utilizing the strong nonlinearity and positive-normal dispersion of a single-mode As_2Se_3 fiber, in combination with a tailored chirped fiber Bragg grating. The value and sign of the dispersion, coupled with the high nonlinearity of the chalcogenide, produces a smoothly broadened spectrum with a monotonic chirp via self phase modulation. Measurements of the phase and time evolution of the laser pulses using frequency resolved optical gating are performed showing excellent agreement with theory. We also discuss the limiting influence of two-photon absorption. © 2006 American Institute of Physics. [DOI: 10.1063/1.2178772]

Simple, compact schemes utilizing novel materials and configurations to generate ultrashort sub-picosecond pulses are of significant interest to experimentalists involved in ultra-fast next generation optical component research. It is desirable to be able to generate ultra-short pulses in a particular wavelength region of interest, for example the C-band for telecommunications research. Generally, the required operation wavelength dictates the materials which may be used for a given compression scheme.

A variety of pulse compression schemes that relies on self-phase modulation (SPM) and dispersion have been demonstrated.¹ Anomalous group velocity dispersion (GVD) of optical fibers can be exploited in soliton-effect compression schemes for very high compression ratios. The resulting pulse quality, however, is generally impaired by the formation of a substantial pulse pedestal. Subsequently, only a fraction of the input pulse energy appears in the compressed pulse.^{2,3} If normal dispersion in a fiber is combined with SPM, the spectrum may be broadened and smoothed out with minimal spectral modulation. By subsequent recompression of the pulse via a suitable anomalous dispersive element, pulses which are potentially pedestal free, may be obtained.⁴

Chalcogenide glass is a promising material that exhibits very strong optical nonlinearities and strong normal dispersion around 1550 nm.⁵ While the extraordinarily strong normal dispersion of chalcogenide glass has previously been regarded as a nuisance,⁶ SPM pulse compression schemes can exploit strong normal dispersion. In this paper, it is shown that the strong normal dispersion of chalcogenide glass fiber, combined with the high optical nonlinearity, can be exploited in a compact, low-power, all-fiber high quality optical pulse compression scheme. First, we take advantage of the high optical nonlinearity and dispersive properties to generate a SPM broadened pulse with a linear frequency chirp at low peak powers. We then demonstrate efficient compression of these chirped pulses using a precisely tailored, chirped fiber Bragg grating (FBG). Experimental measurements of the pulse amplitude and phase, obtained using FROG techniques, are compared with numerical simulations of the nonlinear Schrödinger equation. These results highlight the properties of chalcogenide waveguide systems for optical pulse compression and regeneration in very compact (≈ 4 m long) all-optical devices, in contrast to silica based

fibers, where the low optical nonlinearity means that many 100's of meters of fiber are required for any sizable SPM at moderate peak pulse powers < 1 kW. Moreover, since the dispersion in ordinary single mode fibers is typically anomalous around 1550 nm, they are unsuitable for this compression scheme in wavelength regions of interest to telecommunications research.

Figure 1 is a schematic of the all-fiber optical pulse compression scheme, utilizing a single-mode chalcogenide fiber and a chirped FBG. The measured delay of the FBG is shown in the inset. To investigate the operation of the device, it is useful to define characteristic length scales required for dispersive (L_D) and nonlinear (L_{NL}) effects to play an important role:

$$L_D = \frac{\tau_p^2}{k|\beta_2|} \quad \text{and} \quad L_{NL} = \frac{1}{\gamma \hat{P}} \quad \text{with} \quad \gamma = \frac{2\pi n_2}{\lambda_0 A_{\text{Eff}}}. \quad (1)$$

Here τ_p is the initial full width at half maximum (FWHM) pulse duration, k a constant depending on the pulse shape (1.66 for Gaussian pulses), n_2 the nonlinear refractive index, λ_0 the center wavelength of the laser, A_{Eff} the effective mode area in the fiber and β_2 the group-velocity coefficient (positive for normal dispersion). In the first stage of the nonlinear evolution, the optical pulse undergoes SPM that spectrally broadens the pulse. In the absence of dispersion, the pulse spectrum would develop a strong oscillatory structure, the temporal pulse shape would remain unchanged and the pulse would acquire an extremely nonlinear phase. The role

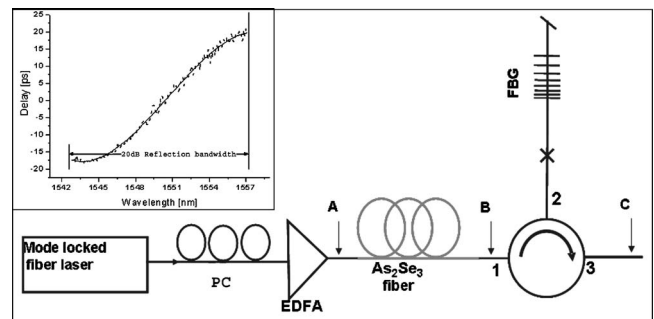


FIG. 1. Experimental setup. PC: polarization control; EDFA: erbium doped fiber amplifier; FBG: fiber Bragg grating. The inset shows the group delay introduced by the fiber Bragg grating and its reflection bandwidth.

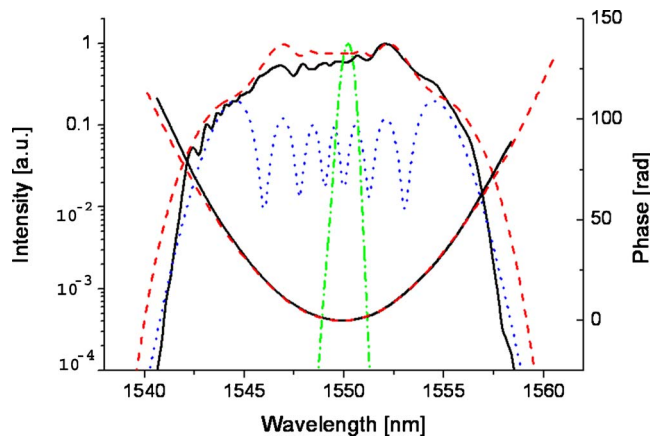


FIG. 2. (Color online) Spectral intensity and phase of the laser pulses after the chalcogenide fiber. Solid line: retrieved from the FROG measurements. Dashed line: Numerical simulations. Dotted: Simulations excluding GVD showing high spectral modulation. Dash-dot: input spectrum.

of the normal GVD is to smooth the spectral broadening and linearize the frequency chirp, which at the same time results in temporal broadening of the pulse. The spectrally and temporally broadened, linearly chirped pulse can be compressed using a linearly dispersive element. The nonlinearity is not needed in the second stage of the compression scheme and in this case, the nonlinearity is over a factor of 1000 less in the short length of silica fiber compared to the chalcogenide fiber. Simple heuristics have been presented to estimate the required fiber length z_{opt} for a given compression ratio F^4

$$F \cong 0.63 \cdot \sqrt{\frac{L_D}{L_{NL}}}, \quad \text{and} \quad z_{\text{opt}} \cong 2.51 \cdot \sqrt{L_D \cdot L_{NL}}. \quad (2)$$

The optimum fiber for this compression technique, therefore, exhibits a high optical nonlinearity n_2 and at the same time, a high and positive dispersion β_2 . Fortunately, chalcogenide waveguides exhibit very large positive values of β_2 at 1550 nm, since their bandgap lies in the far infrared, and they also exhibit extraordinarily high nonlinearities (up to $400\times$ silica glass).

In our experiment, we used a figure-of-eight fiber laser as a pump source, producing 6 ps pulses at a 9 MHz repetition rate and a center wavelength of 1550 nm. The laser was butt-coupled to a 4.1 m long As_2Se_3 chalcogenide fiber. This material exhibits the highest nonlinearity reported so far for an optical fiber.⁷ The peak input power launched into the fiber was estimated to be $\hat{P}=35$ W. To suppress possible cladding modes, we coated the cladding at both ends with gallium.⁸ The mode field diameter of the As_2Se_3 fiber was measured to be around 7 μm .

Figure 2 shows the broadened spectrum at point “B” (Fig. 1), compared to the original laser pulse (dash-dot line). The dashed line is the result of our numerical simulations (see below) whereas the solid line represents the retrieved FROG-data. Note the spectrum has been broadened substantially. In contrast to spectral broadening by SPM in the absence of dispersion where the spectrum is highly modulated with spectral nulls (dotted line), the spectral intensity in the case of this high dispersion is smooth across the whole bandwidth. Moreover, the interplay between SPM and a highly positive dispersion generates an almost perfectly quadratic phase, equivalent to a linear frequency chirp, as can be seen in Fig. 3, where the temporal pulse intensity and chirp at

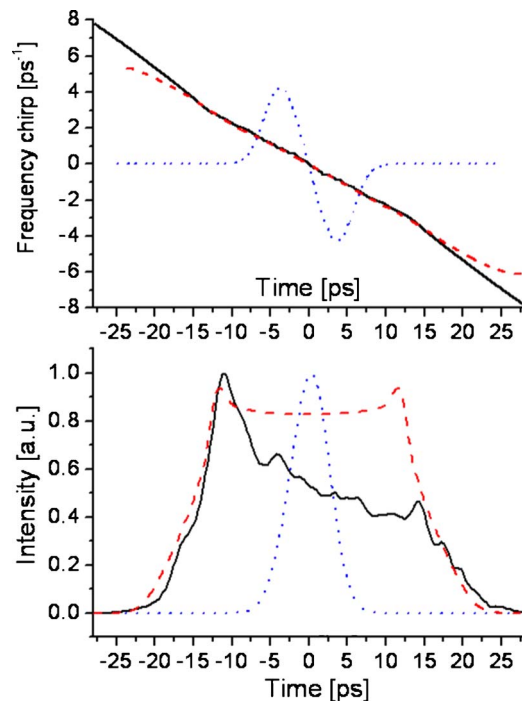


FIG. 3. (Color online) Temporal intensity and phase of the laser pulses after the chalcogenide fiber. Solid line: Retrieved from the FROG measurements. Dashed line: numerical simulations. Dotted: simulations excluding GVD showing highly nonlinear dispersion.

point “B” are shown. The solid line again shows the FROG results and the dashed line the simulations. Note the clear contrast to the GVD-less case (dotted line), where the frequency chirp is highly nonlinear near the pulse edges, making its compensation very difficult, if not impossible.

It is worth noting that the launched peak power value is above the theoretical limit for the onset of Raman gain with CW pumping.⁷ However, the actual permissible power is much higher because GVD leads to a walk-off between the pump pulse and the Stokes pulse which is almost 100 ps for our fiber. Thus, no substantial amount of energy can be transferred to the Stokes wave.

To verify our data, we simulated pulse propagation in the fiber by numerically solving the nonlinear Schrödinger equation (NLSE) using the split-step Fourier method.¹ The fiber dispersion is measured to be $\beta_2=0.71$ ps²/m with a very small slope of $\beta_3=0.03$ ps³/m. The fiber loss was given by the manufacturer to be 1 dB/m, whereas the value for the nonlinear refractive index n_2 and the two-photon absorption (TPA) coefficient β were taken from our previous experiments⁹ to be $n_2=9\times 10^{-18}$ m²/W and $\beta=2.5\times 10^{-12}$ m/W. A measure of the relative influence of TPA, with respect to the nonlinear optical properties in a medium, is the figure-of-merit $\text{FOM}=n_2/(\beta\cdot\lambda)$. We infer a value of 2.3 for our fiber. The excellent agreement between the simulations and the retrieved FROG data gives us confidence in the model and parameters used.

Based on the FROG measurements, we designed a suitable dispersive delay line in order to achieve the highest possible compression ratio. To avoid the bulky and hard to align grating or prism pair, normally used for this task, we opted for an all-fiber based setup. Air-guiding photonic crystal fibers have recently been used for this task.¹⁰ However, they typically also exhibit substantial higher order dispersion and polarization mode dispersion and do not offer the free-

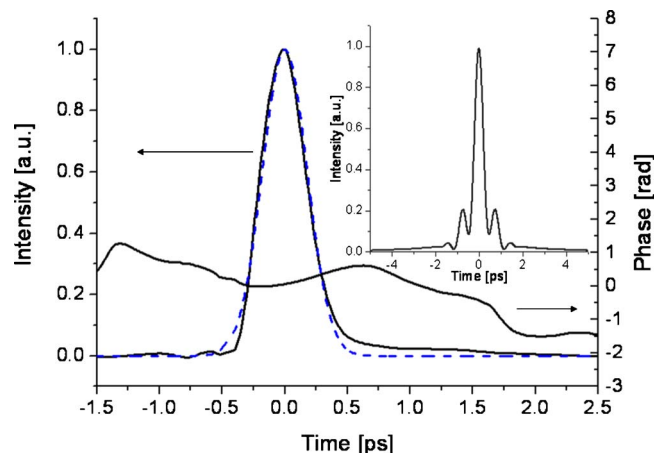


FIG. 4. (Color online) Experimentally generated temporal intensity and phase of the compressed pulses, together with a Gaussian fit to the intensity (dotted line). The inset shows the temporal intensity of the compressed pulse without high GVD in the fiber leading to a considerable pulse pedestal and high temporal sidelobes.

dom to independently tune the second- and third-order dispersion. We, therefore, fabricated an FBG with a chirp matched to, but with opposite sign to, the chirp on the laser pulses. The grating was written with a phase mask into a silica cladding mode suppressed fiber with $\Delta n \approx 10^{-3}$ and a length of about 4 mm. Figure 4 shows the temporal intensity and phase of the pulses after the grating (point “C” in Fig. 1). We achieve a compressed pulse duration of as short as 420 fs ($F=14.3$) with an almost constant phase across the main part of the pulse, i.e., the pulse is almost transform limited. The dotted line represents a Gaussian fit to the measured pulse. As a comparison, the inset shows the temporal intensity of the compressed pulse without the influence of high GVD in the fiber. Pre- and post pulses with an intensity of more than 20% of the main pulse and a very long pedestal are the result of the strong modulations in the spectrum and the noncompressible nonlinear chirped induced by SPM. We want to emphasize that due to the high difference in nonlinearity between chalcogenide and silica fibers, respectively, strong nonlinear optical effects can be utilized in the former, while the FBG written into the latter, still constitutes a linear device. Further power scaling can be realized by employing large mode area fibers for the fabrication of the FBG.¹¹

The ultimate limit in terms of power scaling is given by the onset of TPA in the chalcogenide fiber. In our case, the nonlinear losses are roughly equal to the linear losses (4 dB).

Even higher input power levels, therefore, would lead to a noticeable degradation in the device performance. However, the development of optical fibers based on chalcogenide is still in its infancy. Improved fabrication techniques are anticipated to bring down the linear losses whereas proper bandgap engineering has the potential to reduce TPA. Higher values of the FOM are to be expected for future chalcogenide fibers, allowing for even higher compression ratios using the present technique.

In conclusion, we have experimentally and numerically investigated an extremely compact, all-fiber based scheme for compression of ultra short optical pulses at 1550 nm. Due to the high optical nonlinearity in the As_2Se_3 chalcogenide fiber combined with the high normal dispersion at this wavelength, only 4.1 m of fiber are sufficient to obtain substantial spectral broadening with an almost linear frequency chirp across the pulse. A short simply tailored FBG may be used to compress the pulses to near the transform limit. Chalcogenide based pulse compressors, therefore, represent a promising scheme for the generation of femtosecond laser pulses in a very compact setup.

This work was conducted with the assistance of the Australian Research Council under the ARC Centers of Excellence program. CUDOS (Center for Ultrahigh bandwidth Devices for Optical Systems) is an ARC Center of Excellence.

- ¹Govind P. Agrawal, *Nonlinear Fiber Optics*, 2nd ed. (Academic, San Diego, CA, 1995).
- ²L. F. Mollenauer, R. H. Stolen, J. P. Gordon, and W. J. Tomlinson, *Opt. Lett.* **8**, 289 (1983).
- ³M. A. Foster, A. L. Gaeta, Q. Cao, and R. Trebino, *Opt. Express* **13**, 6848 (2005).
- ⁴W. J. Tomlinson, R. H. Stolen, and C. V. Shank, *J. Opt. Soc. Am. B* **1**, 139 (1984).
- ⁵Y. Ruan, W. Li, R. Jarvis, N. Madsen, A. Rode, and B. Luther-Davies, *Opt. Express* **12**, 5140 (2004).
- ⁶A. Asobe, H. Itoh, T. Miyazawa, and T. Kanamori, *Electron. Lett.* **29**, 1966 (1993).
- ⁷R. E. Slusher, G. Lenz, J. Hodelin, J. Sanghera, L. B. Shaw, and I. D. Aggarwal, *J. Opt. Soc. Am. B* **21**, 1146 (2004).
- ⁸D.-P. Wei, T. V. Galstian, I. V. Smolnikov, V. G. Plotnichenko, and A. Zohrabyan, *Opt. Express* **13**, 2439 (2005).
- ⁹L. B. Fu, M. Rochette, V. G. Ta'eed, D. J. Moss, and B. J. Eggleton, *Opt. Express* **13**, 7637 (2005).
- ¹⁰L. B. Fu, I. C. M. Littler, J. T. Mok, and B. J. Eggleton, *Electron. Lett.* **41**, 306 (2005).
- ¹¹N. G. R. Broderick, D. J. Richardson, D. Taverner, J. E. Caplen, L. Dong, and M. Ibsen, *Opt. Lett.* **24**, 566 (1999).